Indian J. pure appl. Math., **34**(9) : 1315-1326, September 2003

MAGNETIC EFFECT ON PULSATILE FLOW IN A CONSTRICTED AXIS-SYMMETRIC TUBE

E. AMOS

Department of Mathematics, Rivers State University of Science and Technology, PMB 5080, *Port-Harcourt, Nigeria*

AND

A. OGULU

Department of Basic Sciences, Botswana College of Agriculture, Private Bag 0027, *Gaboron, Botswana*

(*Received* 10 *September* 2001; *accepted* 9 *October* 2002; *accepted* 29 *April* 2003)

The paper considers the effect of an externally applied magnetic field on pulsatile flow in constricted arteries. We model the physiological constriction known as stenosis in humans. The leading equations are modelled via the Navier-Stokes equations. Analytical approximations are made at specific locations and the numerical results for the stream function and vorticity are obtained using the Galerkin technique of the finite element method. The accuracy of the numerical solutions of the model was satisfactorily tested against straight tubes without constriction. The results obtained for the velocity and shear stress on the wall are displayed graphically and the effect of the magnetic field discussed quantitatively.

Key Words : Pulsatile Flows; Constricted Axis-Symmetric Tube; Tube

1. INTRODUCTION

The flow of a viscous fluid in a tube of slowly varying section is of fundamental importance with obvious applications not only in physiology but also in engineering. From the physiological point of view, for flow in large arteries blood may be treated as a Newtonian viscous fluid, Manton[10]. For flow in situations other than large arteries, the complex nature of blood has been approximated as a suspension of particles, Kaimal[11]. The mechanics of blood flow in the microcirculation largely determines the workload of the heart.

Literature abound on the flow of blood in tubes with constriction. Chow and Soda[4] looked at laminar flow in tubes with construction to understand the abnormal flow conditions caused by the presence of stenosis in arteries. Rabadi *et al.*[12], studied the effect of pulsatile flow in curved tubes upon heat transfer characteristics. In Gupta and Singh[13] the effect of a transverse magnetic field on oscillatory flow in a curved pipe was studied for different times where it was observed that the effects of magnetic field are more pronounced at larger times. Rao and Deshikachar[14] applied the work of Gupta and Singh[12] to a physiological situation where they observed that the effect of a magnetic field reduces the magnitude of the flow velocity near the central region of the pipe. Deshikachar and Rao[15] looked at the effect of a magnetic field on the flow and blood oxygenation in channels of variable cross-section. Some other workers in this area include McMichael *et al.*[18], Deshikachar and Rao[16], Haldar and Ghosh[2], Tay and Ogulu[17], Ogulu[9]; the list is not exhaustive.

There is abundant evidence that the existence of abnormal flow conditions may not necessarily be as a result of boundary irregularities but also a result of some external influence on the flow regime. From the point of view of fluid mechanics, it has been shown in Ogulu[1] that these boundary irregularities are mainly caused by arterosclerosis (medically known as stenosis in human) and is a disorder arising from a blockage of the blood vessel. The study, further establishes that arterosclerosis is effected by hydro-dynamical conditions imposed on the vascular walls. From medical survey, Haldar and Ghosh[2], it is a well known fact that more than 80% of the total deaths are due to a disease relating to the constriction or blockage of one blood vessel or the other.

The role of a magnetic field in arterial blood flow has been reviewed by many authors. In one such study, Branover[5] established that a magnetic field interacts with the mean average steady flow such that stability is manipulated by chainging the mean flow velocity distributions, and this effect may well be much more significant than a direct separation on disturbance. In other study Ogulu and Alabraba[8] observed that the application of a magnetic field induces a flow potential which is most pronounced in the major blood vessels around the heart and in the heart itself. The work by Lantinopoulos and Ganoulis[6] treated pulsatile flow numerically in continuously perturbed conduit and tubes.

In all the above studies none has applied the Galerkin finite element technique. This present study incorporates the effect of magnetic field in order to understand in general terms the mechanisms of such complicated flow. Specific emphasis is placed on axis-symmetric constriction and Galerkin technique of the finite element method. The analysis has contributed in providing the quantitative data necessary to achieve a better understnading of the basic fluid mechanic phenomena in human circulatory system and that the fundamental theorems evolving from this work has increased the knowledge of haemo-dynamics and cardiovascular response.

2. GOVERNING EQUATIONS

The geometry of arteriosclerotic plaque is not well defined. In this present usage prosthetic devices for cardiovascular use have diverse geometrical characteristics. Therefore, a method to analyse arbitrary shape is developed in this work. A series of bell-shaped constriction in an infinitely long cylindrical tube whose contours are defined by a cosine curve is used. If r is the radial co-ordinate, then for any point on the wall the location varies sinusoidally and is given by:

$$r = R\left(1 - \varepsilon \cos \frac{2\pi z}{L_w}\right) \qquad \ldots (1)$$

where R is the mean radius of the tube, ε is a dimensionless amplitude of the wall. $\frac{2\pi}{L_w}$ is a wave number corresponding to the wavelength of the tube, z is the axial co-ordinate (Fig. 1). As in Latinopoulos and Ganoulis[6], we choose this form of geometry because of the uncertainty about the arterial wall's actual shape as well as for convenience. The beauty of the finite element algorithm used below is that it is capable of dealing with any form of boundaries in the flow field.

To simplify the formulation, we impose the following restrictions:

(*i*) That the walls are rigid and stationary. This is so because in arterosclerotic vascular system where stenosis appears, the vessel walls have already lost part of their elasticity;

(*ii*) that the flow is unsteady and axis-symmetric,

(*iii*) that blood may be treated as a homogeneous, Newtonian viscous fluid. Actually, blood is a suspension of cells in plasma. The plasma, is a solutin of proteins, electrolytes and other substances, is an incompressible, virtually Newtonian fluid. The cells are red blood cells, white blood cells of several different types, and platelets. Normal human blood has a hematocrit (volume fraction

red cells) of about 45% and so red cells strongly influence the flow peoperties of blood. The red cells have a diameter of about 8×10^{-4} cm, and the diameter of arteries in humans ranges from 0.05-0.3 cm, therefore, the homogeneity assumption is tenable. The Newtonian assumption is reasonable since at sufficiently large shear rates, say above 200 sec^{-1}, the blood viscosity is nearly constant, Lee and Fung[7];

(*iv*) that the flow is fully developed and pulsatile varying like

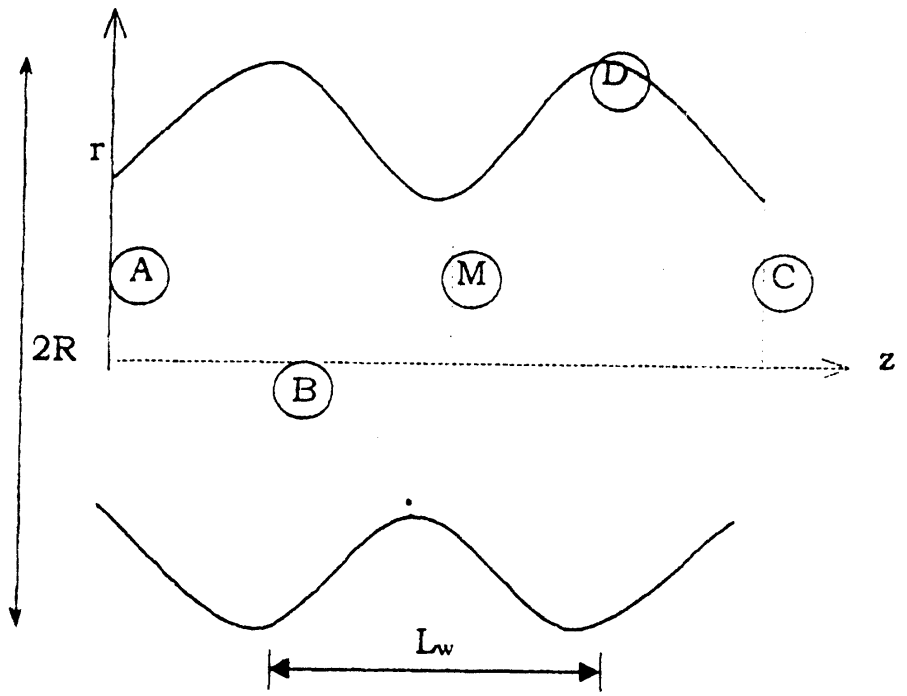

FIG. 1 Schematic representation of the constricted internal passage.

$$R_e = \bar{R}_e (1 + \beta \sin \omega t) \qquad \ldots (2)$$

where $R_e = \bar{U}(t)\frac{R}{\nu}$ is the instantaneous Reynolds number and $\bar{R}_e = \bar{U}(t)\frac{R}{\nu}$ is the steady state Reynolds number, ω is the frequency of oscillation and β is the amplitude factor for which $\beta = 0$ implies steady state and $\beta = 1$ implies fully pulsatile regime,

(*v*) that the magnetic field is uniform and constant in time.

Turning to the idealised mathematical model, we consider a long cylindrical tube with axis-symmetric constriction. Let (r, θ, z) be a set of cylindrical co-ordinates with z-axis coinciding with the axis of the tube. We consider a pulsatile axis-symmetric flow in the region $0 \leq r \leq s(z)$ and $-\infty < z < +\infty$, $s(z)$ will denote conditions at the wall. Then the Navier-Stokes equations where the body force term accounts for the effect of magnetic field only, are presented in dimensional form as :

$$\frac{\partial v'}{\partial t'} + v'\frac{\partial v'}{\partial r'} + u'\frac{\partial v'}{\partial z'} = -\frac{1}{\rho}\frac{\partial P'}{\partial r'} + \nu\left(\frac{\partial^2 v'}{\partial r'^2} + \frac{1}{r'}\frac{\partial v'}{\partial r'} - \frac{v'}{r'^2} + \frac{\partial^2 v'}{\partial z'^2}\right) - \sigma H^2 v' \qquad \ldots (3)$$

$$\frac{\partial u'}{\partial t'} + v' \frac{\partial u'}{\partial r'} + u' \frac{\partial u'}{\partial z'} = -\frac{1}{\rho} \frac{\partial P'}{\partial z'} + \nu \left(\frac{\partial^2 u'}{\partial r'^2} + \frac{1}{r'} \frac{\partial u'}{\partial r'} + \frac{\partial^2 u'}{\partial z'^2} \right) \quad \ldots (4)$$

The fluid is incompressible so that the equation of continuity is

$$\frac{\partial u'}{\partial z'} + \frac{1}{r'} \frac{\partial}{\partial r'} (r' v') = 0 \quad \ldots (5)$$

where v' is the radial velocity, u' is the axial velocity, P' is the pressure, ρ is the density and ν is the kinematic viscosity of the fluid, H is the magnetic field vector and σ represents electrical conductivity. We now introduce the following non-dimensional parameters.

$$z = \frac{z'}{R}, \quad r = \frac{r'}{R}, \quad t = \omega t', \quad u = \frac{u'}{U}, \quad v = \frac{v'}{R}, \quad P = \frac{P'}{\rho \bar{U}^2} \quad \ldots (6)$$

$$M^2 = H^2 R^2 \left(\frac{\sigma}{\nu} \right), \quad \Psi = \frac{\Psi'}{\bar{U} R}, \quad \eta = \frac{\eta'}{\omega}$$

In virtue of eqn. (6) governing eqns. (3-5) become

$$\frac{\alpha^2}{\bar{R}_e} \frac{\partial v}{\partial t} + v \frac{\partial v}{\partial r} + u \frac{\partial v}{\partial z} = -\frac{\partial P}{\partial r} + \frac{1}{\bar{R}_e} \left(\frac{\partial^2 v}{\partial r^2} + \frac{1}{r} \frac{\partial v}{\partial r} + \frac{v}{r^2} + \frac{\partial^2 v}{\partial z^2} \right) - \frac{M^2}{\bar{R}_e} v \quad \ldots (7)$$

$$\frac{\alpha^2}{\bar{R}_e} \frac{\partial u}{\partial t} + v \frac{\partial u}{\partial r} + u \frac{\partial u}{\partial z} = -\frac{\partial P}{\partial z} + \frac{1}{\bar{R}_e} \left(\frac{\partial^2 u}{\partial r^2} + \frac{1}{r} \frac{\partial u}{\partial r} + \frac{\partial^2 u}{\partial z^2} \right) - \frac{M^2}{\bar{R}_e} u \quad \ldots (8)$$

$$\frac{\partial u}{\partial z} + \frac{1}{r} \frac{\partial}{\partial r} (r v) = 0 \quad \ldots (9)$$

In eq. (6), $\bar{U}$ is the steady state mean flow velocity in the mean section of the tube, η is the vorticity, Ψ is the stream function. The parameter α, appearing in eqs. (7) and (8) is usually referred to as the pulsatile Reynolds number or the Wormersley number. It is an essential factor in pulsatile flow and can be defined as :

$$\alpha = R \left(\frac{\omega}{\nu} \right)^{\frac{1}{2}}$$

The parameter α is related to the Reynolds number through the relation

$$S_t = \frac{\alpha^2}{\bar{R}_e}$$

where S_t is the Strauhal number $\left(S_t = \frac{\omega R}{\bar{U}} \right)$.

We now introduce the vorticity function, η and the stream function, Ψ as

$$\eta = -\frac{\partial u}{\partial r} + \frac{\partial v}{\partial z}, \quad u = -\frac{1}{r} \frac{\partial \Psi}{\partial r}, \quad v = \frac{1}{r} \frac{\partial \Psi}{\partial r} \quad \ldots (10)$$

so that eqs. (7) to (9) can be replaced by the vorticity transport equations:

$$\frac{\alpha^2}{\bar{R}_e}\frac{\partial \eta}{\partial t}+\frac{\partial}{\partial z}(u\,\eta)+\frac{\partial}{\partial r}(v\,\eta)=\frac{1}{\bar{R}_e}\left(\frac{\partial^2 \eta}{\partial z^2}+\frac{\partial^2 \eta}{\partial r^2}+\frac{1}{r}\frac{\partial \eta}{\partial r}-\frac{\eta}{r^2}\right)-\frac{M^2}{\bar{R}_e}\eta \qquad \ldots (11)$$

$$\frac{\alpha^2}{\bar{R}_e}\eta=\frac{\partial}{\partial z}\left(\frac{1}{r}\frac{\partial \Psi}{\partial z}\right)+\frac{\partial}{\partial r}\left(\frac{1}{r}\frac{\partial \Psi}{\partial r}\right) \qquad \ldots (12)$$

3. BOUNDARY CONDITIONS

(*i*) Entrance and exit sections (Figure 1, cross-sections at *A* and *C*)

Initially we impose a Poiseuille-type flow at both ends, and then the solution algorithm numerically corrects this initial flow type at every time step guided by eq. (9) and the periodicity in both time and space.

The flow at both ends of the entrance and exit sections are identical and are governed by the equation

$$\frac{\alpha^2}{\bar{R}_e}\frac{\partial u}{\partial t}=-\frac{\partial P}{\partial z}+\frac{1}{\bar{R}_e}\left(\frac{\partial^2 u}{\partial r^2}+\frac{1}{r}\frac{\partial u}{\partial r}\right)-\frac{M^2}{\bar{R}_e}u \qquad \ldots (13)$$

where $$-\frac{\partial P}{\partial z}=k$$

The solution of the entrance and exist cross-sections can now be found by the Frobenus method. First let

$$u=g_0(r)\,e^{it} \qquad \ldots (14)$$

then subject to the conditions

$$u<\infty \text{ on } r=0$$

$$u=0 \text{ on } r=s\,(z)$$

we obtain g_0 as

$$g_0=\frac{\bar{R}_e k}{(M^2+i\,\alpha^2)}\left\{1-\frac{J_0(\lambda r)}{J_0(\lambda s)}\right\} \qquad \ldots (15)$$

where $\lambda^2=M^2+i\,\alpha^2$, J_n is Bessel function of the first kind of order n. Since $v=0$ at these cross sections, differentiating g_0 with respect to r gives the vorticity as follows

$$\eta=\frac{\bar{R}_e k}{(M^2+i\,\alpha^2)}\left(\frac{J_1(\lambda r)}{J_0(\lambda s)}\right) \qquad \ldots (16)$$

The stream function is given by the integral of the velocity across the flow, hence

$$\Psi=\int_0^s g_0(r)\,r+dr+C \qquad \ldots (17)$$

As is common with other flows (see Cheng *et al.*[3]), Ψ is constant at the boundary. However,

$r = 0$ at the centreline. In this study we take $\Psi = -0.2$. Other values of Ψ show no difference in the analysis, so matching this value with the value of r at the centreline we get

$$-0.21 = \frac{\bar{R}_e k}{(M^2 + i\alpha^2)} \left\{ \frac{s^2}{2} - \frac{sJ_1(\lambda s)}{J_0(\lambda s)} \right\} + C \qquad \ldots (18)$$

Therefore the constant is the mean centreline value of the stream function, so that at any point on the inflow or outflow cross-sections

$$\Psi = \int_0^s g_0(r)\, r\, dr + C \qquad \ldots (19)$$

By using eq. (18), eq. (19) becomes

$$\Psi = \frac{\bar{R}_e k}{(M^2 + i\alpha^2)} \left\{ \frac{r^2}{2} - \frac{rJ_1(\lambda s)}{J_0(\lambda s)} \right\} - 0.2 - \left\{ \frac{\bar{R}_e k}{(M^2 + i\alpha^2)} \left(\frac{s^2}{2} - \frac{sJ_1(\lambda s)}{J_0(\lambda s)} \right) \right\} \qquad \ldots (20)$$

(*ii*) Axis of symmetry (see Fig. 1 cross-section B)

Because of symmetry,

$$u = u_{\max}, \quad \eta = -\frac{\partial u}{\partial r} + \frac{\partial v}{\partial z} = 0 \qquad \ldots (21)$$

$v = 0$, Ψ = constant

(*iii*) For the rigid body (Fig. 1, cross-section D)

Velocity vanishes on the rigid boundary, while the stream function has a constant value. To compute η at the wall, we use

$$\eta = \frac{\bar{R}_e k}{(M^2 + i\alpha)^2} \left(\frac{J_1(\lambda r)}{J_0(\lambda s)} \right)_{r = s(z)} \qquad \ldots (22)$$

In each of the boundaries ((i)-(iii)) eq. (2) gives the range for the flow from steady state to a fully pulsatile regime and must therefore be taken note of in the applications.

4. FINITE ELEMENT DISCRETIZATION

We divide the region of concern into triangular elements (see Fig. 2). The collection of triangles is denoted by D and the vertices of the triangles are called nodes. Solutions η_i and Ψ_i at the nodal points as functions of time is used to approximate the constricted flow passage.

Now the flow volume is a body of revolutions and all integrations are referred to this. Therefore because of symmetry about the axis the volume differential can be written as

$$dv = 2\pi r \; dD = 2\pi r\, dz\, dr \qquad \ldots (23)$$

We assume that a set of weighing functions N_η and N_Ψ exist in the integration domain D such that they can take arbitrary values anywhere in D and vanish on the boundary Γ. We are now in a position to apply the Galerkin method, first we multiply eq. (11) and eq. (12) by N_η and N_Ψ respectively to obtain;

$$\frac{\alpha^2}{\bar{R}_e} r^2 N_\eta \frac{\partial \eta}{\partial t} + r^2 N_\eta \frac{\partial}{\partial z}(u\,\eta) + r^2 N_\eta \frac{\partial}{\partial r}(v\,\eta)$$

$$= \frac{N_\eta}{\bar{R}_e}\left(r^2 \frac{\partial^2 \eta}{\partial z^2} + r^2 \frac{\partial^2 \eta}{\partial r^2}\; r\frac{\partial \eta}{\partial r} \right) - \frac{M^2}{\bar{R}_e} r^2 N_\eta \eta \qquad \ldots (24)$$

$$\frac{\alpha^2}{\bar{R}_e} r^2 N_\Psi \eta = r N_\Psi \left(\frac{\partial^2 \Psi}{\partial z^2} + \frac{\partial^2 \Psi}{\partial r^2} \right) - N_\Psi \frac{\partial \Psi}{\partial r} \qquad \ldots (25)$$

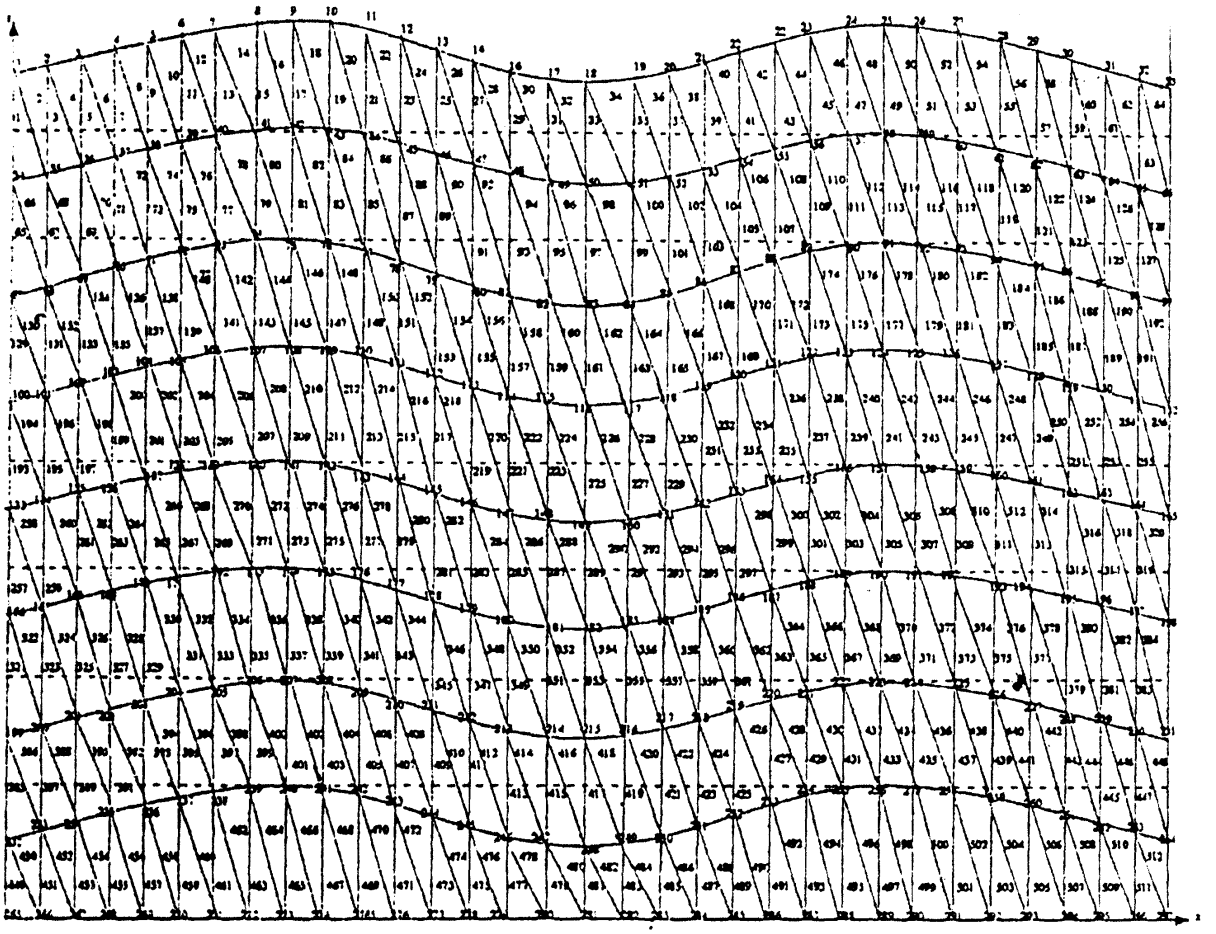

FIG. 2. The finite element grid

Integrating eq. (24) and eq. (25) over the entire volume, using (23) to transform volume differential to $z - r$ plane and making use of Green's theorem we obtain ;

$$\frac{\alpha^2}{\bar{R}_e} \int_D r^2 N_\eta \frac{\partial \eta}{\partial t}\, dD + \int_D r^2 N_\eta \frac{\partial}{\partial z}(u\,\eta)\, dD + \int_D r^2 N_\eta \frac{\partial}{\partial r}(v\,\eta)$$

$$= \frac{1}{\bar{R}_e} \int_D \left\{ -r^2 \frac{\partial N_\eta}{\partial z}\frac{\partial \eta}{\partial z} - r^2 \frac{\partial N_\eta}{\partial r}\frac{\partial \eta}{\partial r} - 2rN_\eta \frac{\partial \eta}{\partial r} + rN_\eta \frac{\partial \eta}{\partial r} - N_\eta \eta \right\} \times dD$$

$$-\frac{M^2}{\bar{R}_e}\int_D r^2 N_\eta\,\eta\,dD \qquad \ldots (26)$$

$$\frac{\alpha^2}{\bar{R}_e}\int_D r^2 N_\Psi\,\eta\,dD = -\int_D \left\{ r\left(\frac{\partial N_\Psi}{\partial z}\frac{\partial \Psi}{\partial z} - \frac{\partial N_\Psi}{\partial r}\frac{\partial \Psi}{\partial r}\right) + 2N_\Psi \frac{\partial \Psi}{\partial r}\right\} dD \qquad \ldots (27)$$

Using linear interpolating functions $\Psi, \eta, N_\Psi, N_\eta$ within every triangle D_m in the entire flow region ($D = \sum_{m=1}^{L} D_m$ L is the number of elements in the region), and assembling the contribution of each element we have:

$$\frac{\alpha^2}{\bar{R}_e}\left(\sum_{m=1}^{L}\int_{D_m} r_m^2 N_{\eta m} N_m\,dD\right)\left(\frac{\partial \eta}{\partial t}\right)_m + \left(\sum_{m=1}^{L}\int_{D_m} r^2 N_{\eta m}\frac{\partial N_m}{\partial z}\,dD_m\right)(u\,\eta)$$

$$+\left(\sum_{m=1}^{L}\int_{D_m} r_m^2 N_{\eta m}\frac{\partial N_m}{\partial r}\,dD_m\right)(v\,\eta)$$

$$+\frac{1}{\bar{R}_e}\left(\sum_{m=1}^{L}\int_{D_m} r^2\left\{ \frac{\partial N_{\eta m}}{\partial z}\frac{\partial N_m}{\partial z} + \frac{\partial N_{\eta m}}{\partial r}\frac{\partial N_m}{\partial r} + M^2 N_{\eta m} N_m\right\} dD_m\right)\eta_m$$

$$+\frac{1}{\bar{R}_e}\left(\Sigma\int\left(r_m N_{\eta m}\frac{\partial N_m}{\partial r} + N_{\eta m} N_m\right) dD_m\right)\eta_m = 0 \qquad \ldots (28)$$

$$\frac{\alpha^2}{\bar{R}_e}\left(\sum_{m=1}^{L}\int_{D_m} r^2 N_{\Psi_m} N_m\,dD_m\right)\eta =$$

$$-\left(\sum_{m=1}^{L}\int_{D_m} r_m\left\{\left(\frac{\partial N_{\Psi_m}}{\partial z}\frac{\partial N_m}{\partial z} + \frac{\partial N_{\Psi_m}}{\partial r}\frac{\partial N_m}{\partial r}\right) + 2N_{\Psi_m}\frac{\partial N_m}{\partial r}\right\} dD_m\right)\Psi_m \qquad \ldots (29)$$

After evaluating the expressions in eq. (28) and eq. (29), we can symbolically write them in matrix form as the global matrices, thus;

$$\frac{\alpha^2}{\bar{R}_e} C\frac{\partial \eta}{\partial t} = -\frac{1}{\bar{R}_e} D\,\eta\,\frac{M^2}{\bar{R}_e} E\,\eta - (F(u\,\eta) + G(v\,\eta)) \qquad \ldots (30)$$

$$H\,\Psi = -\frac{\alpha^2}{\bar{R}_2} K\,\eta \qquad \ldots (31)$$

in which C, D, E, G, H and K denote global matrices and vectors whose dimensions are equal to the total number of nodal points in the flow region, and

$$C = \sum_{m} \int_{D_m} r_m^2 N_{\eta_m} N_m \, dD_m = E$$

$$D = \sum_{m} \int_{D_n} \left\{ r_m^2 \left(\frac{\partial N_{\eta_m}}{\partial z} \partial \frac{N_m}{\partial z} + \frac{\partial N_{\eta_m}}{\partial r} \frac{\partial N_m}{\partial r} \right) + r_m N_{\eta_m} \frac{\partial N_m}{\partial r} + N_{\eta_m} N_m \right| dD_m$$

$$F = \sum_{m} \int_{D_m} r_m^2 N_{\eta_m} \frac{\partial N_m}{\partial z} \, dD_m \qquad \ldots (32)$$

$$G = \sum_{m} \int_{D_m} r_m^2 N_{\eta_m} \frac{\partial N_m}{\partial r} \, dD_m$$

$$H = \sum_{m} \int_{D_m} \left\{ r_m^2 \left(\frac{\partial N_{\Psi_m}}{\partial z} \frac{\partial N_m}{\partial z} + \frac{\partial N_{\Psi_m}}{\partial r} \frac{\partial N_m}{\partial r} \right) + 2 N_{\Psi_m} \frac{\partial N_m}{\partial r} \right\} dD_m$$

$$K = \sum_{m=1} \int_{D_m} r_m^2 N_{\Psi_m} N_m \, dD_m$$

r_m denotes the radial co-ordinate within each triangular element.

5. PROCEDURE FOR THE NUMERICAL SOLUTION

To obtain the solution for the system above we carry out the following steps:

(*i*) we impose the boundary conditions for the stream function on eq. (34). We next pose the boundary condition for the vorticity on eq. (31); we then obtain steady state solutions which form the initial data for the unsteady flow by solving eqns. (33) and (34)

$$-\frac{1}{\bar{R}_e} D\,\eta - \frac{M^2}{\bar{R}_e} E\,\eta = (F(u\,\eta + G(v\,\eta)) \qquad \ldots (33)$$

$$H\,\Psi = -\frac{\alpha^2}{\bar{R}_e} K\,\eta \qquad \ldots (34)$$

and imposing the condition $b\eta = 0$ on eq. (2).

Solutions so obtained for Ψ and η form the initial data for the unsteady flow.

(*ii*) At every time step, we solve eq. (31) for Ψ according to the boundary conditions for the stream function.

(*iii*) We solve eq. (30) for $\frac{\partial \eta}{\partial t}$ according to the boundary conditions for the vorticity and making use of the approximation

$$\frac{\partial \eta}{\partial t} = \frac{\eta_{t+\Delta t} - \eta_t}{\Delta t}$$

(*iv*) The values of Ψ, η, u and v computed at the mid-section (section M of the flow is next

compared to the values at the entry and exist sections. We repeat the procedure if there is a remarkable difference between these values for any of the variables to ensure convergence.

(*v*) Steps (*ii*)-(*iv*) form the unsteady state solution which is repeated for each time step and ranging β from 0.25 – 1 in eq. (2).

6. CALCULATION SPECIFICATIONS

In the computing process, stability criteria established by Latinoupoos and Ganoulis[6] for their axis-symmetric flow was modified for our case. We therefore have them in the form

$$\Delta t \leq \frac{3\,\Delta z^2\,\bar{R}_e}{144 + \bar{R}_e^2\,\Delta z^2}$$

for the steady flow and

$$\Delta t \leq \frac{3\,\Delta z^2\,\alpha^2}{144 + \bar{R}_e^2\,\Delta z^2}$$

for the unsteady flow, where Δz is the mean value of the sides of the triangular element. Calculations were done for a constriction specified by eq. (1) in which $\varepsilon = 0.1, \frac{L_w}{R} = 2$. The profile is bell-shaped and is roughly confined to the interval $z \leq 3.2$.

The iterative algorithm was terminated when

$$| \Psi^k - \Psi^{k-1} | < 10^{-4} \text{ and } | \eta^k - \eta^{k-1} | < 10^{-5}$$

where k is the number of iterations. This condition for the vorticity was not enforced for points near the axis of symmetry where η becomes extremely small.

For a change in Reynolds number, this process was carried out such that the solution at a lower Reynolds number was used as initial condition for a higher Reynolds number in which the range of parameter values for which the scheme converges is up to 400 for the mean Reynolds number, $\bar{R}_e$, and the pulsatile Reynolds number, α, kept at 30. The spacing in the radial and axial directions have proved to be sensitive in the values of the variables $\psi\ \eta, u$ and v. To preserve inter-element continuity the values of u and v are computed through local polynomial approximation of the Ψ-values for each node and making use of eq. (10, b, c).

7. SHEAR STRESS AT THE WALLS

From physical pint of view, it is necessary to know the shear stress tangential to the walls of the tube. They are given by

$$\tau = -\frac{\partial u}{\partial r}\bigg|_{r = s(z)}$$

8. DISCUSSION OF RESULTS AND CONCLUSION

Numerical solution of the governing equations for the magnetic effect on pulsatile flow in a constricted internal passage has been obtained. Difficulties arising from non-linearity of the governing

equations and the complexity of the boundaries involved are remedied by solving the governing equations using the Galerkin technique of the finite element method.

Numerical results for the solution of the governing equations have been obtained for the velocity, wall shear stress, vorticity and stream function. Of these results only the wall shear stress and the velocity are plotted for different values of M and β for a better understanding of the problem since here we are looking at the magnetic effects. The effect of the wall perturbation, ε, and some other parametrs such as the oscillatory Reynolds number, α, and the mean flow rate, Q will form the basis of further studies. It is observed that the application of a uniform magnetic field has a definite effect on the velocity of blood flow. As the magnetic field increases, the velocity decreases (see Figure 3). As the flow ranges from steady state $\beta = 0$ to a fully pulsatile regime, $\beta = 1$, there appears to be an increase in the velocity but still countered by the magnetic effect. Since β does no go beyond 1, a very high increase in magnetic field eventually sets the flow to that of steady state ($\beta = 0$) and the effect still abound. We therefore join Ogulu and Alabraba[8] to conclude that there is a reduction in flow at the entrance of the aorta as a result of the magnetic field effect. A natural way to offset the decrease in velocity is to increase the pressure k. However, as shown in Ogulu[9], increase in the pressure corresponds to an increase in the workload on the heart which is the genesis of cardiac failure (heart attack).

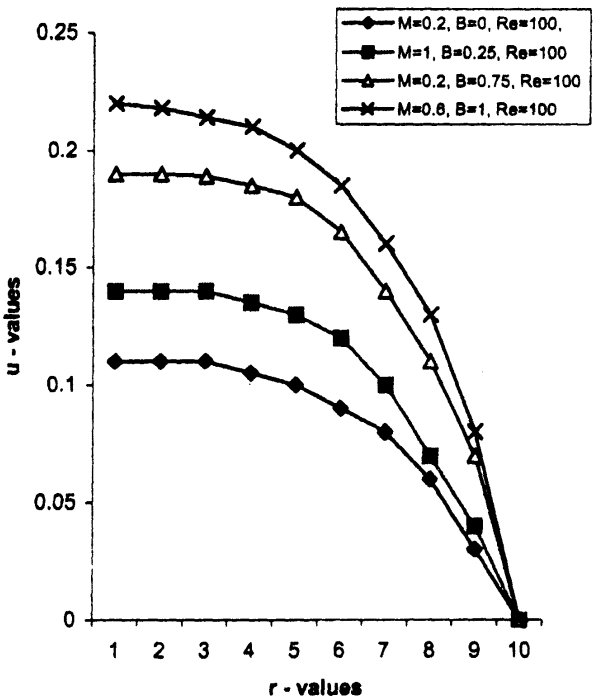

FIG. 3. Velocity profile.

To further exhibit the details of the flow, we observe a sharp increase in shear stress just after the stenosis. The shear stress variation at the wall is shown in Fig. 4, where an increase in the magnetic field results in an increase in the shear stress on the wall. It has been pointed out elsewhere, Halder and Ghosh[2], how decisive the action of the shear stress could be in case of abnormal functioning of the blood vessels. In this constricted vessel, the pulsatile flow decreases the value of the shear stress together with a continuously varying regime. At every values of the magnetic field the shear stress on the wall increases and this may lead to a further weakening of the blood vessel. Ultimately, this may lead to paralysis or sudden death. The flattening of the shear stress profile is a result of the magnetic field.

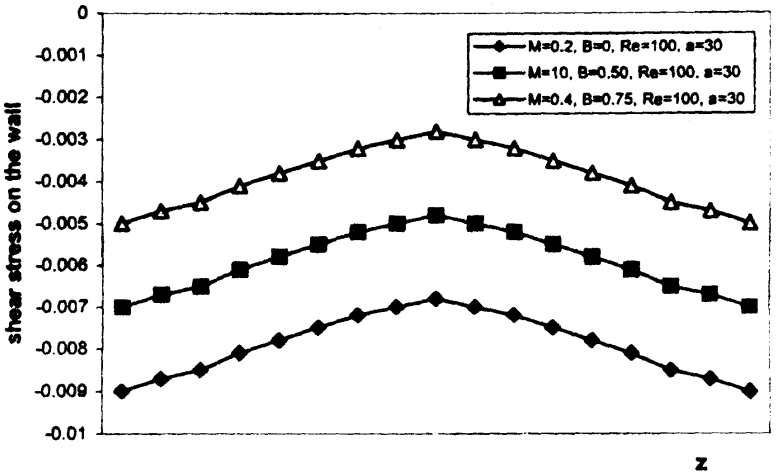

FIG. 4. Shear stress on the wall

In consequence the problem is of interest in the light of biomedical results. Accordingly, the proposed solutions fall within the set of measures to be adopted for an increased knowledge in hemodynamics and cardiovascular response.

ACKNOWLEDGEMENT

The authors would like to acknowledge input from an unknown referee that has improved the quality of this paper.

REFERENCES

1. A. Ogulu, *J. Fiz. Mal.*, **15** (1994), 149.
2. K. Halder and S. N. Ghosh, *Indian J. Pure Appl. Math.*, **25**(3) (1994), 345.
3. L. C. Cheng, M. E. Clark and J. M. Roberts, *J. Bio-mechanics*, **5** (1972), 467.
4. J. C. Chow and K. Soda, *The Physics of fluids*, **15**(10) (1972).
5. H. Branover, *Magneto-hydrodynamic flow in ducts*. John Wiley, New York (1978).
6. P. Latinopoulos and J. Ganoulis, *Appl. Math. Modelling*, **6** (1982), 55.
7. J. Lee and Y. Fung, *Appl. Mech. Trans. ASME*, **37** (1970), 9.
8. A. Ogulu and M. A. Alabraba, *Acta Physica Hungarica*, **72(2-4)** (1992), 223.
9. A. Ogulu, *J. Fiz. Mal.*, **17** (1996), 53.
10. J. Manton, *J. Fluid Mech.*, **49** (1971), 451.
11. M. R. Kaimal, *Inter. J. Engng Sci.*, **17** (1979), 615.
12. N. J. Rabadi, J. C. F. Chow and H. A. Simon, *Int. J. Heat Mass transfer*, **21**(2) (1982), 195.
13. S. C. Gupta and B. Singh, *Physics of Fluids*, **11**(2) February (1970).
14. A. R. Rao and K. S. Deshikachar, *J. Indian Inst. Sci., Jul. - Aug.* **68** (1988), 247.
15. K. S. Deshikachar and A. R. Rao, *Int. J. Engng Sci,*. **23**(10) (1985), 1121.
16. K. S. Deshikachar and A. R. Rao, *Physics of Fluids*, January **30**(1) (1987).
17. G. Tay and A. Ogulu, *J. Fiz. Mal.*, **18** (1997), 105.
18. J. M. McMichael and S. Deutsch, *Physics of Fluids*, January **27**(1) (1984).